




The NCT-WES directional neutron spectrometer: validation of the response with monoenergetic neutron fields

R. Bedogni¹, A. Calamida¹, T. Napolitano¹, C. Cantone¹, A. M. Fontanilla¹, A. I. Castro Campoy¹, G. Abbatini¹, A. Pietropaolo^{2,a} , V. Monti^{3,4}, E. M. Mafucci^{3,4}, M. Bunce⁵, D. Thomas⁵, J.-M. Gomez-Ros⁶, S. Altieri^{7,8}

¹ Istituto Nazionale di Fisica Nucleare, Laboratori Nazionali di Frascati, via Enrico Fermi 40, 00044 Frascati, Italy

² ENEA-Department of Fusion and Technologies for Nuclear Safety and Security, via Enrico Fermi 44, 00044 Frascati, Italy

³ Università degli Studi di Torino, via P. Giuria 1, 10125 Torino, Italy

⁴ INFN, Sezione di Torino, via P. Giuria 1, 10125 Torino, Italy

⁵ National Physical Laboratory, Hampton Road, Teddington TW11 0LW, Middlesex, UK

⁶ CIEMAT, Av. Complutense 40, 28040 Madrid, Spain

⁷ Università degli Studi di Pavia, via Bassi, 6, 27100 Pavia, Italy

⁸ INFN, Sezione di Pavia, via Bassi, 6, 27100 Pavia, Italy

Received: 15 November 2022 / Accepted: 23 February 2023

© The Author(s) 2023

Abstract A directional neutron spectrometer named NCT-WES (Neutron Capture Therapy Wide Energy Spectrometer) was developed for quality assurance of the therapeutic neutron beam in Neutron Capture Therapy (NCT). NCT-WES operates as a “parallelized” Bonner spheres spectrometer, embedding six semiconductor-based thermal neutron detectors in a collimated cylindrical moderator. With the objective of validating the simulation model used to derive its response matrix, irradiations in reference monoenergetic fields were performed at National Physical Laboratory (UK). As the energy distributions of neutron beams in NCT extend from keV to a few MeV, monoenergetic fields in this domain were chosen, namely 71.5 keV, 144.2 keV, 565.1 keV, 841.9 keV and 1200.4 keV. The results of the experiment confirm the correctness of the NCT-WES simulation model, within an overall uncertainty lower than $\pm 2\%$.

1 Introduction

The introduction of commercially available, hospital-sized, particle accelerator-based neutron sources is drawing an increased interest in Boron Neutron Capture Therapy (BNCT). As recommended by the BNCT expert group of IAEA, the spectrum of the therapeutic neutron beam should be measured at the “beam port” [1]. Among the neutron spectrometers being proposed for this purpose so far, NCT-WES (Neutron Capture Therapy Wide Energy Spectrometer) [2] exhibits the broadest energy interval, from thermal energy up to about 10 MeV. Being a single moderator spectrometer [3, 4], it simultaneously provides the whole spectrometric information and thus is able to operate as a continuous spectrometric monitor. As explained elsewhere [2], NCT-WES embeds six thermal neutron detectors in a collimated cylindrical moderator with weight of about 35 kg. Overall, NCT-WES mimics a set of six Bonner Spheres, but its response is sharply directional, and it can operate in real time. The neutron spectrum is obtained by unfolding the readings of the internal detectors with the corresponding response matrix. As the energy distributions of neutron beams in BNCT extend from keV to a few MeV, NCT-WES was designed to have its maximum resolving power in this domain. Similarly to Bonner Spheres, the resolving power of a single moderator spectrometer is higher in energy regions where the degree of differentiation between the response functions of different internal detectors is higher. Although NCT-WES response was already validated in a reference $^{241}\text{Am-Be}$ field, additional validation measurements in monoenergetic epithermal fields are required, in view of its use in BNCT. The validation experiment described in this work was organized at the National Physical Laboratory (NPL) and involved the following reference monoenergetic fields: 71.5 keV, 144.2 keV, 565.1 keV, 841.9 keV and 1200.4 keV.

2 Experimental setup

The irradiation tests took place in the low-scatter irradiation room of NPL, using the 3.5 MV Van de Graaff accelerator operated by the Neutron Metrology Group. The $^7\text{Li}(p,n)$ reactions were exploited to generate 71.5 keV, 144.2 keV, 565.1 keV neutrons, while $\text{T}(p,n)$ was used to generate 841.9 keV and 1200.4 keV neutrons. All measurements were taken at 0° angle with respect to the

NCT-WES response.

^a e-mail: antonino.pietropaolo@enea.it (corresponding author)

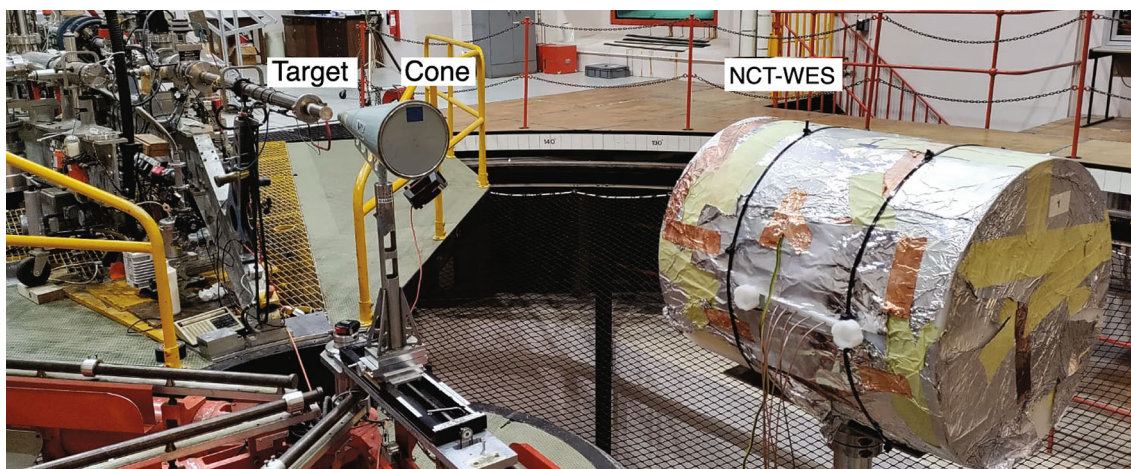


Fig. 1 The experimental setup in the low-scatter irradiation room of NPL. The shadow-cone is in place

Table 1 Irradiation conditions. E_n is the monochromatic neutron energy, R the reaction, u_ϕ is the standard uncertainty on neutron fluence at SDD. TSF is given as percentage of the total fluence

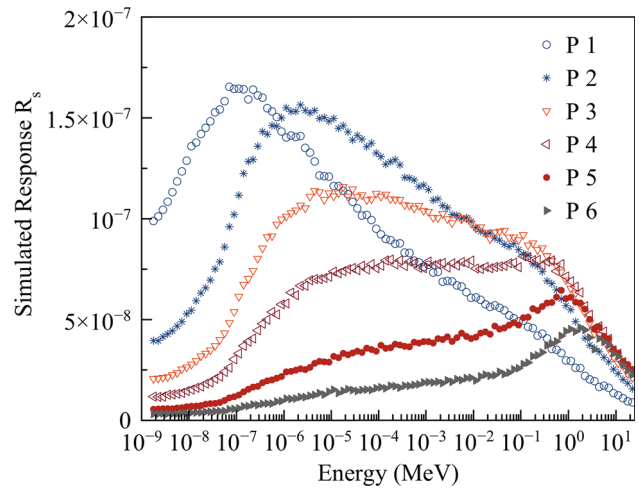
E_n (MeV)	FWHM (keV)	R	Angle	u_ϕ (%)	TSF	SDD (cm)
71.5 ± 4.2	26	${}^7\text{Li}(p,n)$	50	$\pm 4.4\%$	1.7%	180.7
144.2 ± 4.6	29	${}^7\text{Li}(p,n)$	0	$\pm 2.9\%$	1.1%	181.0
565.1 ± 3.6	19	${}^7\text{Li}(p,n)$	0	$\pm 2.7\%$	0.6%	230.8
841.9 ± 11.6	77	T(p,n)	50	$\pm 2.3\%$	3.6%	180.6
1200.4 ± 14.8	98	T(p,n)	0	$\pm 2.3\%$	3.6%	180.7

direction of the accelerated proton beam, except at 71.5 keV and 841.9 keV, where an angle of 50° was used. The distance from the target to the front face of NCT-WES, henceforth indicated as SDD (source-to-detector distance) ranged from 180 to 230 cm. The shadow-cone technique was used to subtract the air- and room-scatter contribution from the spectrometer readings. The set up can be seen in Fig. 1. The reference value of monoenergetic neutron fluence delivered to the reference point (front face of NCT-WES) was known from measurements performed by means of the Standard NPL long counter in addition to a suite of permanent monitor instruments. The main characteristics of the used beams are summarized in Table 1. The target scatter fraction (TSF), based on Monte Carlo simulations carried out at NPL, can be assumed as affected by uncertainty up to $\pm 40\%$ [5]. These target scattered neutrons have a lower energy than the corresponding monoenergetic ones. Since the long counter, used to determine the reference monoenergetic fluence, has a flat energy dependence of the fluence response, then the result is a slight overestimation of the monoenergetic fluence. This was taken into account in data analysis, as explained in Sect. 4. As described in Ref. [2], the internal thermal neutron detectors of NCT-WES are 1-cm^2 windowless p-i-n diodes coated with $30\ \mu\text{m}$ of ${}^6\text{LiF}$, henceforth named TNPD (thermal neutron pulse detector) [6, 7]. These are located along the NCT-WES cylindrical axis at different distances from the spectrometer front face, namely: 20.22 (shallowest detector in position P1), 21.52, 22.82, 24.12, 26.12 and 28.12 cm (deepest detector in position P6). The signals from the TNPD detectors are recorded using a custom six-channel analog board, each channel including a charge preamplifier of type CREMAT CR-110 and a shaper amplifier of type CREMAT CR-200 with time constant $2\ \mu\text{s}$. As a method to reduce the noise in the analog signal, detectors are inversely biased to 12 V. According to dedicated C-V measurements, this corresponds to a junction capacitance of about 100 pF. Its impact on the amplified signal noise is only 4–5 mV RMS. This is very small, if compared to the amplitude of the neutron signals. As explained in Ref. [8], the genuine neutron-induced events are discriminated from those induced by photons by comparing the pulse height with a threshold, fixed at 0.6 V. The neutron-induced pulse height distribution (PHD) in the TNPD extends in amplitude from this threshold up to about 3 V, with an energy-pulse amplitude conversion factor of about $1\ \text{V} \cdot \text{MeV}^{-1}$. A commercial digitizer (NI USB 6366), operating in streaming mode under customized software written in LabView, allows the data to be recorded on a laptop. For the experiment here described, the “neutron counts” of each TNPD were obtained by integrating the PHD from 0.6 V to 3 V.

3 Computational

The spectrometer was modeled using MCNP 6 [9]. The ENDF/B-VIII [10] neutron cross-sectional libraries below 20 MeV and room-temperature cross-sectional tables in polyethylene, $S(\alpha,\beta)$ were used. The density of polyethylene moderator was measured for each part of the spectrometer, and found to vary between 0.95 and $0.96\ \text{g cm}^{-3}$. Each part was modeled using its own density.

Fig. 2 Simulated Response of NCT-WES at SDD = 180 cm in terms of expected number of pulses per emitted neutron. Symbols P1 to P6 indicate the detector positions from the shallowest to the deepest



A number of histories was used to provide less than 0.5% uncertainty in the results. The internal thermal neutron detectors were modeled in detail, according to Ref. [7]. The scored quantity was the number of (n, t) reactions in the ⁶LiF radiator of the TNPD detectors. This was converted into a “simulated” number of pulses by multiplying by the average TNPD efficiency, or scaling factor, $F = (0.238 \pm 0.006) \frac{\text{pulses}}{(n,t)\text{reaction}}$. F was previously determined by calibrating the device with a reference ²⁴¹Am-Be field [2]. An isotropic point source was positioned at the SDD values specified in Table 1 for each beam. Its energy distribution was assumed to be Gaussian with the average energy and FWHM values listed in Table 1. This allowed calculating the spectrometer response R_s , in terms of counts per emitted neutron, as a function of:

- the neutron energy;
- the detector position;
- the SDD.

It is worth mentioning that the response functions were calculated in a 103 groups equilogarithmic energy structure, including the monoenergetic energies used in the experiment. As an example, R_s at SDD = 180 cm is plotted in Fig. 2. The numerical values of R_s for the SDD and monoenergetic energies used in the experiment are given in Table 2. Here, the uncertainties on R_s are derived as the quadratic combination of the following sources:

- the statistical uncertainty from the Monte Carlo simulation (about $\pm 0.5\%$).
- SDD: an uncertainty of ± 1 cm in the spectrometer positioning was assumed, providing a relative uncertainty on R_s of $\pm 2 \times (1/\text{SDD}) \simeq 1\%$. Indeed, for small variations of SDD, R_s varies as $(\text{SDD} + d_i)^{-2}$, where d_i is the distance from the spectrometer front face to the detector position. This is demonstrated in Figs. 3 and 4, respectively, showing: a. Figure 3: the response R_s of detectors P1 and P6 for SDD varying from 170 to 190 cm. Clearly, R_s depends on SDD. b. Figure 4: the value of $R_s \times (\text{SDD} + d_i)^2$ for detectors P1 and P6 and for SDD varying from 170 to 190 cm. For a given detector, $R_s \times (\text{SDD} + d_i)^2$ does not depend on SDD.
- The uncertainty on the peak energy, ranging from less than $\pm 1\%$ (565.1 keV) up to $\pm 6\%$ (71.5 keV). The impact of this uncertainty on R_s was evaluated by simulation.
- The uncertainty on F ($\pm 2.5\%$).

4 Results and discussion

For a given monochromatic irradiation, the measured NCT-WES response, R_m , was derived for every detector, as follows:

$$R_m = \frac{C_{i,tot}}{N_{Tot}} - \frac{C_{i,cone}}{N_{cone}} \tag{1}$$

The symbols in Eq. (1) represent:

- $C_{i,tot}$ and $C_{i,one}$ the neutron counts (integral the PHD from 0.6 V to 3 V) in the i -th position in the total field and shadow-cone irradiations, respectively;
- N_{tot} and N_{cone} the number of monoenergetic neutrons emitted by the target if the emission was isotropic.

Fig. 3 Simulated Response R_s at SDD = 170, 180 and 190 cm for detectors P1 and P6

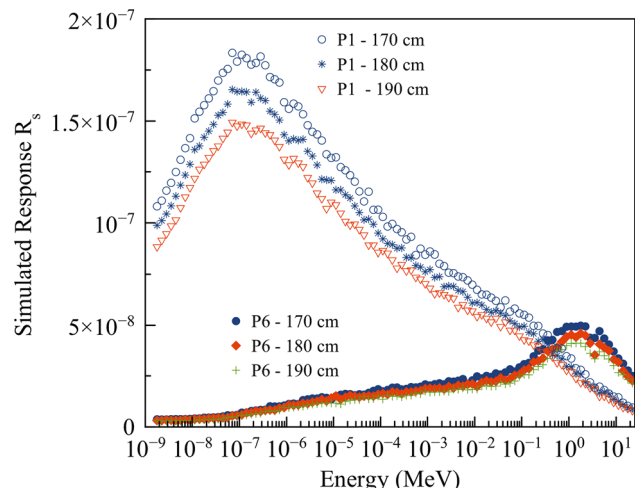
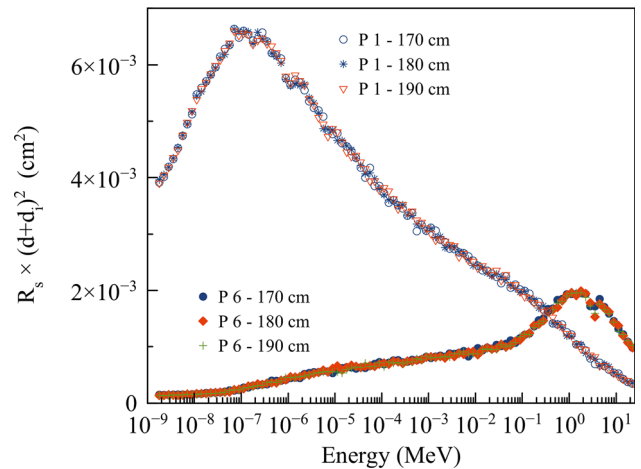


Fig. 4 Product $R_s \times (SDD+d_i)^2$ at SDD = 170, 180 and 190 cm for detectors P1 and P6. For a given detector, this product does not depend on SDD



Clearly the monoenergetic neutron emission from a target is not isotropic in terms of fluence or energy. Nevertheless, the NCT-WES collimator has 12 cm diameter and is positioned at about 2 m from the target. Thus, the subtended solid angle is so small that the neutron field across this surface can be considered uniform in fluence and energy. N_{tot} and N_{cone} are calculated by:

$$N = \Phi \cdot (1 - TSF) \cdot 4\pi \cdot SDD^2 \tag{2}$$

where Φ is the neutron fluence. The R_m values for the studied monoenergetic beams are reported in Table 2, where the R_s/R_m quotient, q , is also reported. A good agreement between simulation and experiment was obtained, the q values always being compatible with one (uncertainties are 1 standard deviation). The thirty values of $q_{i,E}$ (where i denotes the detector position and E the monoenergetic energy) are scattered with a s.d. of about 4%. If they are combined in a weighted mean, using the inverse square of uncertainties as weights, the best estimation of q is $q_{best} = (1.002 \pm 0.008)$. If the matrix given in Table 2 is analyzed per columns, a weighted mean over the position can be calculated. The resulting q_E values, reported in the end of each column, are energy-dependent. All q_E values are very near to one, denoting no systematic errors depending on the energy. If for example the fluence monitoring was affected by a bias in a specific energy, the corresponding q value could significantly deviate from one for that energy. If the matrix is analyzed per rows, a weighted mean over the energy is achieved. The resulting q_i values, reported in the end of each row, are position-dependent. Compared to the q_E values, the q_i values are more scattered. This depends on small detector-to-detector differences in terms of thermal neutron efficiency, or amount of ^6LiF radiator coating. However, being these deviations always lower or equal to 2 s.d., no detector-specific correction will be applied. Thus, the NCT-WES simulation model proved to be very accurate and its overall uncertainty, studied as a function of the energy or detector position, is always lower or equal to $\pm 2\%$.

5 Conclusions

NCT-WES is a prototypal neutron spectrometer with directional response, which design was optimized for the application in BNCT. Its applicability as workplace spectrometer was previously verified in the MeV region [11]. The NCT-WES simulation model,

Table 2 NCT-WES response in terms of counts per emitted neutron as a function of the neutron energy and the detector position: simulated (R_s), measured (R_m) values, and their ratio q . Energy- and position-average q values are also reported

	E (keV)	71.5	144.2	565.1	841.9	1200.4	q_i
	SDD (cm)	180.7	181.0	230.8	180.6	180.7	
P1	$R_s(\times 10^{-8})$	5.13 ± 0.33	4.69 ± 0.20	2.25 ± 0.07	3.15 ± 0.10	2.80 ± 0.09	
	$R_m(\times 10^{-8})$	4.85 ± 0.22	4.43 ± 0.14	2.20 ± 0.06	3.07 ± 0.08	2.79 ± 0.07	1.03 ± 0.02
	q	1.06 ± 0.08	1.06 ± 0.06	1.02 ± 0.04	1.03 ± 0.04	1.00 ± 0.04	
P2	$R_s(\times 10^{-8})$	8.53 ± 0.56	8.03 ± 0.34	4.05 ± 0.11	5.79 ± 0.18	5.17 ± 0.16	
	$R_m(\times 10^{-8})$	8.22 ± 0.37	7.69 ± 0.24	4.08 ± 0.12	5.78 ± 0.15	5.13 ± 0.13	1.01 ± 0.02
	q	1.04 ± 0.08	1.04 ± 0.05	0.99 ± 0.04	1.00 ± 0.04	1.01 ± 0.04	
P3	$R_s(\times 10^{-8})$	9.00 ± 0.59	8.75 ± 0.37	4.82 ± 0.14	7.03 ± 0.22	6.38 ± 0.20	
	$R_m(\times 10^{-8})$	8.53 ± 0.39	8.14 ± 0.25	4.68 ± 0.13	6.79 ± 0.17	6.31 ± 0.16	1.03 ± 0.02
	q	1.06 ± 0.08	1.07 ± 0.06	1.03 ± 0.04	1.04 ± 0.04	1.01 ± 0.04	
P4	$R_s(\times 10^{-8})$	7.73 ± 0.50	7.88 ± 0.33	4.80 ± 0.13	7.23 ± 0.23	6.72 ± 0.21	
	$R_m(\times 10^{-8})$	7.78 ± 0.35	7.77 ± 0.24	5.04 ± 0.14	7.41 ± 0.19	7.10 ± 0.18	0.97 ± 0.02
	q	0.99 ± 0.08	1.01 ± 0.05	0.95 ± 0.04	0.98 ± 0.04	0.95 ± 0.04	
P5	$R_s(\times 10^{-8})$	4.77 ± 0.31	5.17 ± 0.22	3.82 ± 0.11	6.10 ± 0.19	5.98 ± 0.18	
	$R_m(\times 10^{-8})$	4.63 ± 0.21	4.93 ± 0.15	3.86 ± 0.11	5.84 ± 0.15	5.81 ± 0.15	1.03 ± 0.02
	q	1.03 ± 0.08	1.05 ± 0.06	0.99 ± 0.04	1.04 ± 0.04	1.03 ± 0.04	
P6	$R_s(\times 10^{-8})$	2.53 ± 0.17	2.90 ± 0.12	2.56 ± 0.07	4.36 ± 0.14	4.52 ± 0.14	
	$R_m(\times 10^{-8})$	2.74 ± 0.13	3.00 ± 0.09	2.75 ± 0.08	4.40 ± 0.11	4.69 ± 0.12	0.96 ± 0.02
	q	0.92 ± 0.07	0.96 ± 0.05	0.93 ± 0.04	0.99 ± 0.04	0.96 ± 0.04	
	q_e	1.01 ± 0.03	1.03 ± 0.02	0.984 ± 0.016	1.011 ± 0.017	0.991 ± 0.016	

required in future to generate the workplace-specific response matrix, was here benchmarked using metrology-grade monoenergetic neutron beams from 71 to 1200 keV. Its overall uncertainty, studied as a function of the energy or detector position, is always lower or equal to $\pm 2\%$. Next steps will be testing NCT-WES in a clinical BCNT beam, and its adoption by the BNCT community as a routine tool for the quality assurance of the therapeutic beams.

Funding Open access funding provided by Ente per le Nuove Tecnologie, l'Energia e l'Ambiente within the CRUI-CARE Agreement.

Data Availability Statement This manuscript has associated data in a data repository. [Authors' comment: The data sets generated during and/or analyzed during the current study are available from the corresponding author on reasonable request].

Open Access This article is licensed under a Creative Commons Attribution 4.0 International License, which permits use, sharing, adaptation, distribution and reproduction in any medium or format, as long as you give appropriate credit to the original author(s) and the source, provide a link to the Creative Commons licence, and indicate if changes were made. The images or other third party material in this article are included in the article's Creative Commons licence, unless indicated otherwise in a credit line to the material. If material is not included in the article's Creative Commons licence and your intended use is not permitted by statutory regulation or exceeds the permitted use, you will need to obtain permission directly from the copyright holder. To view a copy of this licence, visit <http://creativecommons.org/licenses/by/4.0/>.

References

- (Draft) Report of the IAEA Virtual Technical Meeting on, Advances in Boron Neutron Capture Therapy, IAEA Headquarters, Vienna, Austria 27-31 July (2020)
- R. Bedogni, A. Lega, A. Calamida, V. Monti, A.I. Castro-Campoy, L. Menzio, T. Napolitano, A. Pola, D. Bortot, A. Pietropaolo, M. Costa, S. Altieri, *Europhys. Lett.* **134**, 42001 (2021)
- R. Bedogni, J.M. Gomez-Ros, D. Bortot, A. Pola, M.V. Introini, A. Esposito, A. Gentile, G. Mazzitelli, B. Buonomo, *Eur. Phys. J. Plus* **130**, 24 (2015)
- A. Pietropaolo, M. Angelone, R. Bedogni, N. Colonna, A.J. Hurd, A. Khaplanov, F. Murtas, M. Pillon, F. Piscitelli, E.M. Schooneveld, K. Zeitelhack, *Phys. Rep.* **875**, 1 (2020)
- National Physical Laboratory, NPL, Test Report **N2121**(2020020444), 12 (2022)
- R. Bedogni, D. Bortot, A. Pola, M.V. Introini, M. Lorenzoli, J.M. Gomez-Ros, D. Sacco, A. Esposito, A. Gentile, B. Buonomo, M. Palomba, A. Grossi, *Nucl. Instr. Meth. A* **780**, 51 (2015)
- R. Bedogni, A. Calamida, I. Castro-Campoy, J.M. Gomez-Ros, A. Lega, M. Moraleda, A. Pietropaolo, S. Altieri, *Nucl. Instr. Meth. A* **1018**, 165855 (2021)
- R. Bedogni, D. Bortot, B. Buonomo, A. Esposito, J.M. Gomez-Ros, M.V. Introini, M. Lorenzoli, A. Pola, D. Sacco, *Nucl. Instr. Meth. A* **767**, 159 (2014)
- C.J. Werner (Ed.), *MCNP Users' Manual - Code Version 6.2*, Report LA-UR-17-29981, Los Alamos National Laboratory (USA, 2017)
- D.A. Brown et al., *Nucl. Data Sheets* **148**, 1 (2018)
- R. Bedogni, A. Calamida, A. Fontanill, A.I. Castro Campoy, T. Napolitano, C. Cantone, E. Mafucci, V. Monti, S. Altieri, J.M. Gomez-Ros, M. Pillon, A. Pietropaolo, *Eur. Phys. J. Plus.* **137**, 773 (2022)